Published in final edited form as:
Neuroimage. 2013 November 15; 82: 154–159. doi:10.1016/j.neuroimage.2013.05.112.

The Cruciform model of striate generation of the early VEP, re-illustrated, not revoked: a reply to Ales et al (2013)

Simon P. Kelly[a,b,*], **M. Isabel Vanegas**[a], **Charles E. Schroeder**[c,d], and **Edmund C. Lalor**[e,f,g]

[a]Department of Biomedical Engineering, City College of New York, New York, NY 10031, USA [b]Program in Cognitive Neuroscience, City College of New York, New York, NY 10031, USA [c]Cognitive Neuroscience and Schizophrenia Program, Nathan Kline Institute for Psychiatric Research, 140 Old Orangeburg Road, Orangeburg, NY 10962, USA [d]Department of Psychiatry, Columbia University College of Physicians and Surgeons, 1051 Riverside Drive, New York, NY 10032, USA [e]School of Engineering, Trinity College Dublin, Dublin 2, Ireland [f]Trinity Centre for Bioengineering, Trinity College Dublin, Dublin 2, Ireland [g]Trinity College Institute of Neuroscience, Trinity College Dublin, Dublin 2, Ireland

Abstract

Here we summarize the points raised in our dialogue with Ales and colleagues on the cortical generators of the early visual evoked potential (VEP), and offer observations on the results of additional simulations that were run in response to our original comment. For small stimuli placed at locations in the upper and lower visual field for which the human VEP has been well characterized, simulated scalp projections of each of the visual areas V1, V2 and V3 invert in polarity. However, the empirically measured, earliest VEP component, "C1," matches the simulated V1 generators in terms of polarity and topography, but not the simulated V2 and V3 generators. We thus conclude that, 1) consistent with the title of Ales et al (2010a), polarity inversion on its own is not a sufficient criterion for inferring neuroelectric sources in primary visual cortex; but 2) inconsistent with additional claims made in Ales et al (2010a), the simulated topographies provide additional evidence for – not against – the tenet that the C1 component is generated in V1.

In Ales et al (2010a), scalp topographies resulting from activation of discrete visual areas V1, V2 and V3 were simulated based on retinotopic mapping data of 27 subjects. Consistent with the known projections of the lower visual field to the dorsal, mostly upward-facing division of V2/V3, and of the upper field to the ventral, mostly downward-facing division (Wandell et al., 2009), they found that simulated V2/V3 scalp topographies inverted in polarity for upper and lower locations. Upper-lower field polarity inversion is one of the more popularly known properties of the earliest component of the human visual evoked potential (VEP), "C1" (e.g. Martinez et al., 1999; Di Russo et al., 2002) and one of several properties comprising the classic "cruciform model" which proposes a primary visual cortical (V1) source for the C1 (Jeffreys and Axford, 1972a,b; Clark et al., 1995). Combined with the results of constrained source modeling from another study indicating simultaneous onset of V1 and V2 (Ales et al., 2010b), Ales et al. (2010a) took this extrastriate polarity inversion as evidence that the C1 may be generated in V2 and/or V3 rather than in V1. In our original comment (Kelly et al., 2013) we contested this claim, specifically criticizing 1) their critically incomplete definition of the cruciform model, 2) their inappropriate use of

Corresponding author: Simon P Kelly, Department of Biomedical Engineering, The City College of New York, 160 Convent Avenue, New York, NY 10031, USA. 212 650 8626, skelly2@ccny.cuny.edu.

large stimuli that blur V1-consistent topographical shifts, and 3) their neglect of intracranial findings in non-human primates. In their reply, Ales et al (2013) contest the first issue on the basis of the neuroanatomical literature, and remedy the second and third issues by showing the results of new simulations of smaller appropriately-placed stimuli, and by reviewing the relevant human and non-human literature. In the following, we first examine the new simulation results with reference to empirical data for the same visual field locations (Di Russo et al., 2002); we then discuss the systematic within-quadrant topographical shifts that form a critical but neglected part of the unabridged cruciform model, and illustrate them using population-averaged VEP data and anatomical MRI; finally, we briefly address some of the conclusions made by Ales et al. (2013) on the non-human primate literature.

1. The Di Russo et al locations: simulated versus measured

The results of the new simulations of Ales et al. (2013) replicate their previous finding that the scalp-projected potentials resulting from activation of V2 and V3 exhibit clear polarity inversion for stimuli in the upper and lower field. This confirms that polarity inversion cannot be used as the sole criterion in inferring a V1 source, an error that Ales et al claim was made in at least one previous study (Slotnick et al., 1999). Our issue was not with this finding, but rather with the additional finding that V1 projections *do not* polarity invert, and the consequent implication that the empirically observed, polarity-inverting C1 component might be generated in V2 and/or V3 *and not* V1. Ales et al. (2010a) specifically stated that only 3 out of 54 hemispheres showed polarity inversion for V1, although no quantitative criterion was specified for their classification. In their reply to our comment, Ales et al. (2013) have persisted in claiming that V1 responses do not exhibit polarity inversion. Since polarity inversion is the most well-known property of the C1, this directly implies that V1 is not the dominant generator of the C1. It is the latter implication that we examine further here.

Ales et al's (2013) new simulations on the first 10 subjects' data employ the exact same visual field locations as the study of Di Russo et al. (2002), a study in which the waveforms and topographies of the C1 are shown particularly clearly. A direct comparison can now be made between the simulated V1, V2 and V3 topographies and those of normative empirical data, allowing us to address the simple question: given the simulation results, is the empirically measured C1 best explained by a V1 source, a V2 source or a V3 source?

As we predicted, Ales et al's (2013, fig 1) new simulations in V1 show a much clearer polarity inversion for the Di Russo et al locations, which are specifically aimed at the ceiling and floor of the calcarine sulcus in the average brain. Ales et al. (2013) variously state that these simulated topographies "do not fully" or more frankly, "do not" polarity invert, again without specifying any criterion. However, in a large midline scalp region where the C1 is typically measured for these locations, the simulated V1 responses most certainly do invert in polarity (see their fig. 1). As Ales et al. (2013) correctly point out, the complementary positive and negative foci in the simulated topographies coincide more precisely for V2/V3 than for V1. We would further point out that the manner in which the positive and negative V1 foci do not precisely coincide closely parallels empirical C1 measurements (Di Russo et al., 2002; see also Clark et al., 1995 and Kelly et al., 2008 for locations of nearby polar angle). As detailed in Di Russo et al. (2002; see table II, and figures 4, 5 and 6), the upper-field stimuli evoke a negative C1 focus that is slightly ipsilateral to the midline. This ipsilateral effect, mentioned in Jeffreys and Axford (1972) and observed on the individual subject level (Clark et al., 1995, Kelly et al., 2008), can be explained in the cruciform model by the fact that the activated section of cortical surface on the calcarine floor, if not perfectly horizontally-oriented, would naturally tend to face the medial direction on average (refer to coronal section in Fig. 2b). Consistent with the same principle, lower field stimuli in the Di

Russo et al configuration evoke a marked *contralateral*, positive scalp focus. In Ales et al's (2013) simulated responses to the Di Russo et al locations, the V1 topographic foci follow this very pattern, while the simulated V2/V3 responses show very distinct distributions, with upper stimuli clearly projecting to contralateral rather than ispilateral scalp sites (see summary table 1).

More fundamental than these topographical lateralization effects is the fact that the simulated V2/V3 topographies are opposite in polarity with respect to the V1 topographies. The cruciform model not only predicts upper-lower polarity inversion, but more specifically maps the upper field to negative polarity and the lower field to positive polarity for V1 sources, following a surface-negative assumption for initial cortical activation. As we pointed out in our original comment, surface-negative activation of V2/V3 would result in positive scalp polarity for upper stimuli and negative scalp polarity for lower stimuli, which is opposite to the pattern seen for the empirically measured C1. In their figure 1, Ales et al (2013) chose to simulate surface-positive cortical activation rather than surface-negative activation, so that the polarity on the scalp for V2/V3 activation matches the C1. However, surface-positive activation is inconsistent with available intracranial data in monkeys (e.g. Schroeder et al 1991, 1998) and, as we demonstrate in the next section, the within-quadrant topographical shifts observed for the empirical C1 are uniquely consistent with surface-negative activation. If we accordingly assume surface-negative activation for Ales et al's (2013) figure 1, as was done in their figure 3 (note the opposite color of equivalent topographies in figs 1 and 3), the simulated scalp polarities would be as listed in table 1. When considered alongside empirically measured C1 characteristics, these simulation outcomes suggest a very clear winner for the most likely dominant generator of the C1.

In their figure 3, Ales et al. (2013) simulate mixtures of V1 and V2 activity in order to make the point that the polarity of the C1 does not isolate V1 activity because it allows for a 50–50 mixture of V1 and V2. However, when one considers the full scalp distributions rather than just midline electrodes, a comparison between Ales et al's (2013) figure 3 and Di Russo et al's (2002) figure 5 (identical left visual field locations) is very revealing: the Di Russo et al C1 topographies at 70–85 ms closely match the simulated 100%-V1 topographies, whereas the Di Russo et al topographies at 95–115 ms bear a remarkable resemblance to the simulated 50–50 mixture of V1 and V2. Not having the data ourselves, we can only make these comparisons by eye; nevertheless, we would strongly encourage the reader to do the same. Though we agree that it is unlikely that V2 lies inactive for any more than a few milliseconds following the onset of V1 activation, these qualitative comparisons suggest, at least superficially, that V2's expression on the scalp may not come to be as strong as that of V1 until tens of milliseconds after VEP onset.

2. The full Cruciform model includes within-quadrant topographical shifts and a surface-negative assumption

In our original comment, we complained that the definition of the Cruciform model used by Ales et al. (2010a) was a critically truncated one, because it ignored systematic topographic shifts occurring within visual quadrants (Jeffreys and Axford, 1972a). In this section we illustrate why this is important. The full Cruciform model describes a shift from a roughly vertical dipolar orientation on the floor or ceiling of the calcarine sulcus to a roughly horizontal orientation on emergence from the sulcus onto the medial-facing wall, which corresponds to visual locations closer to the vertical meridian (See Clark et al. 1995). As Ales et al (2013) point out, the proportion of V1 lying outside the calcarine sulcus may not be 50%, as was falsely suggested by our casual expression, "as much outside the calcarine sulcus as inside," but rather somewhere between 33% (Hinds et al., 2008) and 45% (Aine et al., 1996). These proportions are still far from negligible, and as we demonstrate below,

these medial-facing sections comprise a very salient part of the full cruciform model that clearly distinguish V1 contributions from V2/V3 contributions.

To first illustrate the above-mentioned within-quadrant topographical shifts, Figure 1 shows the scalp topographies of integrated amplitude in an early (75–85 ms) time interval of a pattern-pulse multifocal VEP (PPMVEP; James 2003) averaged across 16 subjects. The PPMVEP was derived for each of 32 equal-sized radial segments of a large annular checkerboard pattern extending from 3 to 10 degrees of eccentricity (see Vanegas et al., 2013). The main feature to note here is that in every quadrant, as one proceeds from the horizontal meridian toward the vertical meridian, the topography undergoes a shift in orientation consistent with the emergence from the calcarine sulcus, transitioning from a focus close to the midline, consistent with a vertically-oriented dipolar field, to a lateralized pattern consistent with a horizontally-oriented dipolar field. Can this be explained instead by a V2 or V3 source?

In figure 2 we illustrate how the predicted topographical shifts for polar angles nearing the vertical meridian differ for V1 and V2. We took an oblique slice through a population-averaged anatomical image (the MNI-152 brain at 0.5 mm resolution available with AFNI; Cox, 1996) which passes through the standard site POz (20% of the distance from inion to nasion on the scalp according to the 10–20 system), where the Di Russo et al. (2002) C1 components are maximal, and the point along the calcarine sulcus closest to fMRI activations reported in two studies using the same locations (Di Russo et al., 2002, 2007; we converted from Talairach to MNI coordinates using functions from http://www.brainmap.org/icbm2tal/). An outline of the outer surface of the cortex in this slice is rendered in figure 2b, resolving the calcarine sulcus but skipping over other sulci on the outer surface for simplicity. It should be echoed here that individual anatomy varies extremely widely about this average brain; the rounded surface is intended not to be representative of any individual but of the population-average cortical surface, which corresponds with the population-averaged VEP data on which our arguments are based. At this posterior location, the dorsal and ventral V1-V2 borders lie at medially facing sections within the interhemispheric fissure, whereas the V2-V3 borders lie on the outer dorsal or ventral surface. Based on the coincident but opposite-polarity topographies for simulated dorsal and ventral V2 (Ales et al., 2013), we can assume that the lower and upper Di Russo et al locations must project to sections of V2 that are out on the dorsal and ventral surface, respectively, in the average brain. We illustrate the predicted topographical shifts for V1 and V2 using the upper right visual field quadrant as an example, but the logic applies equally well to all quadrants.

Ales et al. (2013) pointed out that while the available evidence in monkeys indicates that the initial cortical activation of both V1 and V2 results in negative potential deflections on the cortical surface, stimulus and species differences preclude the generalization of this finding to contrast-change stimuli in humans. Further, a constrained source modeling study indicated that V2 initially activates with a surface-positive deflection (Ales et al 2010b; but see Hagler et al., 2009). Thus, the negative midline focus for the upper Di Russo et al location (location A in figure 2c) could arise either from surface-negative electric fields in ventral V1 (dipole A in figure 2d), or, alternatively, from surface-positive electric fields in ventral V2 (dipole A in figure 2e). As figures 2d and 2e show, as one proceeds from the horizontal meridian to the vertical meridian (from location A to location B in figure 2c), a shift in dipolar orientation from vertical to horizontal would be predicted for V2 as well as for V1. However, the direction of dipole rotation is opposite for the V1 and V2 cases. In the V1 case, the dipole rotates clockwise, leading to a rightward shift of the negative scalp focus (figure 2f), which is indeed what is seen in empirical data (see figure 1 and Clark et al., 1995). If, instead, the negative upper-field C1 were generated by surface-positive activation

in ventral V2, the dipole would rotate counterclockwise and thus the negative focus would shift towards the left on the scalp (figure 2g), moving in the direction opposite the empirical C1 data.

Thus, in terms of topographical shifts for locations proceeding towards the vertical meridian, the prediction for V2 generation is directly opposite to the prediction for V1, and the empirical data follow the latter. For area V3 and beyond, there are no reported systematic changes in cortical orientation within quadrant representations that could explain the empirical data. Again, we cannot claim that V2 and V3 are entirely inactive during the time frame of these topographies, but it is clear that the V1 contribution must dominate. The potential issue under discussion has been that V2 or V3 activity could potentially masquerade as V1 activity, and so effects on the C1, such as those resulting from attention, may not be on V1 at all. But as we have just seen, for a V2 activation to masquerade as a V1 activation, it would have to be both upside-down and come from a visual cortex that is turned inside-out.

Another visible feature in the empirical data of figure 1 is that the flip in polarity from negative to positive occurs some distance below the horizontal meridian. The distance in these data appears somewhat less than the 20 degrees reported by Clark et al. (1995), but the 32 non-overlapping segments used in this experiment do not offer fine enough resolution to accurately judge. As Ales et al. (2013) point out, more work needs to be specifically aimed at this question to validate Clark et al's (1995) revision of the cruciform model whereby the horizontal meridian projects to a point along the ventral calcarine bank rather than precisely at the fundus. For the time being, we would point out that Ales et al. (2013) did not provide anatomical evidence that was inconsistent with this feature, they merely highlighted that there is a *lack* of evidence that is *consistent* with it, because no functional imaging studies have been specifically aimed at the question. We would further point to a recent study by Benson et al. (2012) that again does not specifically address this question, but nonetheless displays clear images that suggest a horizontal meridian projection to a point ventral to the fundus (see their supplementary figure 1).

To clarify our original position, we at no point claimed that V1 could be fully "isolated" by any means, whether by polarity inversion at certain locations or by timing. Our main point, which we believe is supported by the above arguments, was that the topographical variations in C1 as a function of polar angle are more consistent with a V1 source than a V2 or V3 source, and that even though it is unlikely that V1 is active for long in complete isolation, the evidence suggests that it is by far the dominant contributor to the C1.

3. Insights from intracranial neurophysiology

Ales et al. (2013) provide a literature review on the issues related to intracranial findings, which serves to highlight the uncertainty yet surrounding the inter-area timing, physiological generating mechanisms and scalp projection of early visual activity, and the impact of stimulus and inter-species differences. The authors quite correctly point out that more work needs to be done to resolve these issues. To clarify our original position, we at no point claimed that monkey intracranial data have closed the case on the sequence of activation of visual areas – we merely aired the reasonable complaint that this literature should not be ignored. Further, we did not assert that areas beyond V1 sat in complete silence for the duration of the initial afferent response in V1 – rather, we argued that in light of the current evidence on V1 versus V2 latency differences from intracranial recordings, the finding in human source analysis of simultaneous activation of V1 and V2 should be interpreted with caution.

In the accounting of interareal latency findings in monkey intracranial studies, a couple of critical factors must be considered. First, several studies recorded from anesthetized subjects, a factor which dramatically changes the entire brain response by generally depressing responses and significantly delaying them. Moreover, these effects are distinctive for many of the different anesthetics. This concern applies to numerous empirical as well as review papers; for example, Lamme and Roelfsema (2000) mixed across anesthetized/awake data in a meta-analysis. Second, as Ales et al., (2013) point out, stimulation conditions differ considerably across studies, and care must be taken in mixing these conditions in any meta-analysis.

Among the papers that we cited in our original comment, those that record latencies from the input to the superficial layers of V1 (Schroeder et al., 1991; Givre et al., 1995; Maunsell and Gibson, 1992; Schroeder et al., 1998; Chen et al., 2007) are consistent in showing a significant latency offset. The papers that examine latencies across areas (e.g., Schroeder et al., 1998; Chen et al., 2007) are consistent in showing an offset between areas V1 and V2; very fast responses in V2 due to the magnocellular pathway from the lateral geniculate nucleus (LGN) to 4cα of V1 to the thick CYTOX stripes of V2 does not seem to cause the mass of V2 to respond at a very short latency. The fact that a branch of this pathway does seem to cause a very fast response in the dorsal stream beginning at MT (Chen et al., 2007), and as well may trigger small early responses in V4 (Givre et al., 1994), does not seem relevant to the present dialogue, as these areas do not have polarity-opposed upper-field and lower-field projections and thus could not contribute to the polarity inversion effect. Overall, the studies that have directly compared V1 to V2 have all shown a significant latency difference, despite the caveat that some of the studies show an overall latency increase due to anesthesia (spiking: Raiguel et al., 1989; Nowak et al., 1995; Schmolesky et al., 1998; LFP: Schroeder et al., 1998; Mehta et al 2000). Nowak et al. (1999) state, “Measurements of visual response latencies show that, on average, V2 neurons are activated 10 ms later than neurons in area V1 (Raiguel et al. 1989; Nowak et al. 1995a).” Schmolesky et al. (1998) also showed a delay from V1 to V3, albeit a small one of 6–9 ms. On the whole, despite the stimulus differences, it seems reasonable to say that among the three visual areas identified as having dorsal and ventral sections of opposed orientation, V1, V2 and V3, the available evidence suggests that V1 responds earlier. We would also reiterate that relative response strength should be taken into account - to what degree are areas beyond V1 expressing their activation on the scalp compared to V1? The only studies that directly compare the postsynaptic electrical activation profiles for multiple visual areas in the same monkeys are those of Schroeder et al. (1998), and they show not only earlier, but much stronger (approximately 6x) initial activation in V1 than V2. Undoubtedly, extrastriate areas do not remain silent throughout the initial afferent V1 activation, but at the same time, the “substantial extrastriate contributions” found in human source modeling work (Ales et al., 2010b) may not be definitive.

A final point of Ales et al. (2013) that we are compelled to address is their assertion that response onset latencies for a given stimulus type are equal in humans and non-human primates, and therefore that the 3/5 rule for comparing latencies in monkeys and humans may not be generally applicable. We could not agree less with this assertion. That there is a considerable interspecies difference in neural response latency has been established in a long line of studies from the 60’s to the 90’s. The mean initial V1 response latencies to diffuse flash stimuli, quantified in both spiking and synaptic current flow/local field potentials in unanesthetized monkeys, are between 25 and 30 ms (Schroeder et al., 1998; Maunsell and Gibson, 1992; Chen et al., 2007). Ales et al., (2013) state that such very early (30 ms) onsets in humans have been found both extracranially (Odom et al 2009) and intracranially (Ducati et al., 1988). However, neither of the cited studies were specifically aimed at the issue of response latency and accordingly do not even specify methods for computing latency. Odom

et al. (2009) is a paper about clinical recording standards, which does not specify the stimulation and recording methods used for the example waveforms shown, let alone address common confounds associated with flash stimulus generation, such as early auditory responses to sounds emitted by the stimulation apparatus. Ducati et al., (1988) show response waveforms for both flash and pattern reversal stimuli but do not attempt to precisely measure or directly compare latencies across these stimulus conditions, presumably because non-stimulus evoked activity precludes a clear measurement of onset. An early component, P40 (onsetting around 30ms), was indeed observed in early studies of the flash VEP, but this very small early deflection was believed to be of subcortical origin on the basis of comparisons between human and monkey recordings (Vaughan, 1965, 1966; Kraut et al., 1985). Indeed, Schroeder et al (1992) showed that the early surface component, N25, in the monkey (onset 18–22 ms), could be explained by an intracranial component measured in the lateral geniculate nucleus (LGN). Thus, early-onset components of the human flash VEP can be seen to correspond to even earlier subcortical components in monkeys following the same 3/5 rule.

Ales et al (2013) also claim that pattern-reversal response onsets are equal in human and monkey, on the basis of one human intracranial study reporting latencies of 45–55 ms in recordings made directly from the peri-calcarine region (Farrell et al., 2007). Neither Ales et al., (2013) nor Farrell et al (2007) themselves specify whether this latency range refers to component onset or peak, or whether it was evoked by pattern onset, pattern reversal or flash. Farrell et al. (2007) do point to an N55 component, which they note is on very rare occasions observed as a positive “P55” on the scalp for pattern reversal stimulation. A similarly rare intracranial component “N40” has been reported in the V1 recordings of Schroeder et al., (1991), again consistent with the 3/5 rule. The 3/5 rule not only fits for the aforementioned early visual components but also the pattern-evoked P1 (peaks in monkey at ~60 ms, and in human at ~100 ms), as well as for initial auditory and somatosensory component comparisons (Peterson et al., 1995; Schroeder et al., 1995; Schroeder et al., 2004). Finally, we would reiterate that precise estimates of human V1 onset latencies based on noninvasive measures (Foxe and Simpson, 2002: Clark et al., 1995) come in at about 42–45 ms, consistent with a 3/5 simian/human rule. While the 3/5 principle could use further validation, we introduced it in our discussion in order to emphasize that the latency offsets between V1 and higher visual areas that have been well established in monkeys are likely to be an underestimate of those in humans, and that the overwhelming evidence for V1-V2 latency offsets simply cannot be ignored when interpreting human electrophysiological responses.

To conclude, we emphasize that we have not claimed to know how to isolate, or to have a better “diagnostic,” of V1, nor have we asserted that the cruciform model is infallible. Our main point is that a demonstration of V2/V3 polarity inversion does not constitute strong evidence against the full Cruciform model for primary visual cortical generation of the early VEP. The simulations of Ales et al (2010a, 2013) have clarified a very important aspect of the cruciform model, which is that it is composed of several instances of polarity inversion and topographical shifts with polar angle, and no single instance should be used as a sole diagnostic for a V1 source. Our discussion centered on what this means for the tenet that the earliest component of the VEP is generated in V1, and we have contended that there is no more evidence to the contrary than there was before these simulations were run – in fact, comparisons with empirical data appear to favor the C1-V1 link.

More generally, our discussion should serve as a strong cautionary note in relation to the growing toolkit of the human neurophysiologist. In the present situation, the quantitative sophistication of modern source analysis algorithms has clearly not outweighed the fundamental logic underlying a qualitative model based on elementary geometry and

empirical data. Combined EEG and fMRI approaches building on the remarkable innovations of Ales et al. (2010a,b) and others (e.g. Hagler et al. 2009; Hagler and Dale 2013) will undoubtedly be key in the future use of human visual evoked potentials in understanding visual processing. As we progress, however, it is important not to cast away existing qualitative models as "old notions," but rather incorporate them as logical constraints.

Acknowledgments

Research reported in this publication was supported by the National Institute Of General Medical Sciences of the National Institutes of Health under Award Number SC2GM099626.

References

Aine CJ, Supek S, George JS, Ranken D, Lewine J, Sanders J, Best E, Tiee W, Flynn ER, Wood CC. Retinotopic organization of human visual cortex: departures from the classical model. Cereb Cortex. 1996; 6:354–361. [PubMed: 8670663]

Ales JM, Yates JL, Norcia AM. V1 is not uniquely identified by polarity reversals of responses to upper and lower visual field stimuli. NeuroImage. 2010a; 52:1401–1409. [PubMed: 20488247]

Ales J, Carney T, Klein SA. The folding fingerprint of visual cortex reveals the timing of human V1 and V2. NeuroImage. 2010b; 49 (3):2494–2502. [PubMed: 19778621]

Ales J, Yates JL, Norcia AM. On determining the intracranial sources of visual evoked potentials from scalp topography: A reply to Kelly et al. 2013; 64:703–711.

Benson NC, Butt OH, Datta R, Radoeva PD, Brainard DH, Aguirre GK. The retinotopic organization of striate cortex is well predicted by surface topology. Curr Biol. 2012; 22(21):2081–2085. [PubMed: 23041195]

Chen CM, Lakatos P, Shah AS, Mehta AD, Givre SJ, Javitt DC, Schroeder CE. Functional anatomy and interaction of fast and slow visual pathways in macaque monkeys. Cereb Cortex. 2007; 17:1561–1569. [PubMed: 16950866]

Clark VP, Fan S, Hillyard SA. Identification of early visual evoked potential generators by retinotopic and topographic analyses. Hum Brain Mapp. 1995; 2:170–187.

Cox RW. AFNI: Software for Analysis and Visualization of Functional Magnetic Resonance Neuroimages. Computers and Biomedical Research. 1996; 29 (3):162–173. [PubMed: 8812068]

Di Russo F, Martínez A, Sereno MI, Pitzalis S, Hillyard SA. Cortical sources of the early components of the visual evoked potential. Hum Brain Mapp. 2002; 15:95–111. [PubMed: 11835601]

Di Russo F, Pitzalis S, Aprile T, Spitoni G, Patria F, Stella A, Spinelli D, Hillyard SA. Spatiotemporal analysis of the cortical sources of the steady-state visual evoked potential. Hum Brain Mapp. 2007; 28:323–334. [PubMed: 16779799]

Ducati A, Fava E, Motti ED. Neuronal generators of the visual evoked potentials: intracerebral recording in awake humans. Electroencephalogr Clin Neurophysiol. 1988; 71:89–99. [PubMed: 2449338]

Farrell DF, Leeman S, Ojemann GA. Study of the human visual cortex: direct cortical evoked potentials and stimulation. J Clin Neurophysiol. 2007; 24:1–10. [PubMed: 17277570]

Foxe JJ, Simpson GV. Flow of activation from V1 to frontal cortex in humans. A framework for defining "early" visual processing. Exp Brain Res. 2002; 142:139–150. [PubMed: 11797091]

Givre SJ, Schroeder CE, Arezzo JC. Contribution of extrastriate area V4 to the surface-recorded flash VEP in the awake macaque. Vis Res. 1994; 34:415–438. [PubMed: 8303826]

Givre SJ, Arezzo JC, Schroeder CE. Effects of wavelength on the timing and laminar distribution of illuminance-evoked activity in macaque V1. Vis Neurosci. 1995; 12:229–239. [PubMed: 7786845]

Hagler DJ Jr, Halgren E, Martinez A, Huang M, Hillyard SA, Dale AM. Source estimates for MEG/EEG visual evoked responses constrained by multiple, retinotopically-mapped stimulus locations. Hum Brain Mapp. 2009; 30:1290–1309. [PubMed: 18570197]

Hagler DJ Jr, Dale AM. Improved method for retinotopy constrained source estimation of visual-evoked responses. Hum Brain Mapp. 2013; 34:665–683. [PubMed: 22102418]

Hinds OP, Rajendran N, Polimeni JR, Augustinack JC, Wiggins G, Wald LL, Diana Rosas H, Potthast A, Schwartz EL, Fischl B. Accurate prediction of V1 location from cortical folds in a surface coordinate system. Neuroimage. 2008; 39:1585–1599. [PubMed: 18055222]

James C. The pattern-pulse multifocal visual evoked potential. Invest Ophthalmol Vis Sci. 2003; 44:879–90. [PubMed: 12556425]

Jeffreys DA, Axford JG. Source locations of pattern-specific components of human visual evoked potentials. I. Component of striate cortical origin. Exp Brain Res. 1972a; 16:1–2. [PubMed: 4646539]

Jeffreys DA, Axford JG. Source locations of pattern-specific components of human visual evoked potentials. II Component of extrastriate cortical origin. Exp Brain Res. 1972b; 16:22–40. [PubMed: 4646540]

Kelly SP, Gomez-Ramirez M, Foxe JJ. Spatial attention modulates initial afferent activity in human primary visual cortex. Cereb Cortex. 2008; 18:2629–2636. [PubMed: 18321874]

Kelly SP, Schroeder CE, Lalor EC. What does polarity inversion of extrastriate activity tell us about striate contributions to the early VEP? A comment on Ales et al (2010). NeuroImage. 2013; 76:442–445. [PubMed: 22504764]

Kraut MA, Arezzo JC, Vaughan HG Jr. Intracortical generators of the flash VEP in monkeys. Electroencephalography and Clinical Neurophysiology. 1985; 62:300–312. [PubMed: 2408876]

Lamme VA, Roelfsema PR. The distinct modes of vision offered by feedforward and recurrent processing. Trends Neurosci. 2000; 23(11):571–9. [PubMed: 11074267]

Martínez A, Anllo-Vento L, Sereno MI, Frank LR, Buxton RB, Dubowitz DJ, Wong EC, Hinrichs H, Heinze HJ, Hillyard SA. Involvement of striate and extrastriate visual cortical areas in spatial attention. Nat Neurosci. 1999; 2:364–369. [PubMed: 10204544]

Maunsell JH, Gibson JR. Visual response latencies in striate cortex of the macaque monkey. J Neurophysiol. 1992; 68:1332–1344. [PubMed: 1432087]

Mehta AD, Ulbert I, Schroeder CE. Intermodal selective attention in monkeys. I: distribution and timing of effects across visual areas. Cereb Cortex. 2000; 10:343–358. [PubMed: 10769247]

Nowak LG, Munk MH, Girard P, Bullier J. Visual latencies in areas V1 and V2 of the macaque monkey. Vis Neurosci. 1995; 12:371–384. [PubMed: 7786857]

Nowak LG, Munk MH, James AC, Girard P, Bullier J. Cross-correlation study of the temporal interactions between areas V1 and V2 of the macaque monkey. J Neurophysiol. 1999; 81 (3): 1057–1074. [PubMed: 10085333]

Odom JV, Bach M, Brigell M, Holder GE, McCulloch DL, Tormene AP, Vaegan. ISCEV standard for clinical visual evoked potentials (2009 update). Doc Ophthalmol. 2009; 120:111–119. [PubMed: 19826847]

Peterson NN, Schroeder CE, Arezzo JC. Neural generators of early cortical somatosensory evoked potentials in the awake monkey. Electroencephalogr Clin Neurophysiol. 1995; 96:248–60. [PubMed: 7750450]

Raiguel SE, Lagae L, Gulyàs B, Orban GA. Response latencies of visual cells in macaque areas V1, V2 and V5. Brain Res. 1989; 493 (1):155–159. [PubMed: 2776003]

Schmolesky MT, Wang Y, Hanes DP, Thompson KG, Leutgeb S, Schall JD, Leventhal AG. Signal timing across the macaque visual system. J Neurophysiol. 1998; 79:3272–3278. [PubMed: 9636126]

Schroeder CE, Tenke CE, Givre SJ. Subcortical contributions to the surface-recorded flash-VEP in the awake macaque. Electroencephalogr Clin Neurophysiol. 1992; 84:219–231. [PubMed: 1375881]

Schroeder CE, Tenke CE, Givre SJ, Arezzo JC, Vaughan HG Jr. Striate cortical contribution to the surface-recorded pattern-reversal VEP in alert the monkey. Vision Res. 1991; 31:1143–1157. [PubMed: 1891808]

Schroeder CE, Molholm S, Lakatos P, Ritter W, Foxe JJ. Human-simian correspondence in the early cortical processing of multisensory cues. Cognitive Processing. 2004; 5:140–151.

Schroeder CE, Steinschneider M, Javitt DC, Tenke CE, Givre SJ, Mehta AD, Simpson GV, Arezzo JC, Vaughan HG Jr. Localization of ERP generators and identification of underlying neural processes. Electroencephalogr Clin Neurophysiol Suppl. 1995; 44:55–75. [PubMed: 7649056]

Schroeder CE, Mehta AD, Givre SJ. A spatiotemporal profile of visual system activation revealed by current source density analysis in the awake macaque. Cereb Cortex. 1998; 8:575–592. [PubMed: 9823479]

Slotnick SD, Klein SA, Carney T, Sutter E, Dastmalchi S. Using multistimulus VEP source localization to obtain a retinotopic map of human primary visual cortex. Clin Neurophysiol. 1999; 110:1793–1800. [PubMed: 10574294]

Vanegas MI, Blangero A, Kelly SP. Exploiting individual primary visual cortex geometry to boost steady state visual evoked potentials. J Neural Eng. 2013; 10 (3):036003. [PubMed: 23548662]

Vaughan, HG, jr. The perceptual and physiological significance of visual evoked responses recorded from the scalp in man. In: Burian, HM.; JACOBSON, JH., editors. Clinical Electroretinography. Oxford: Pergamon; 1966.

Vaughan HG jr, Hull RC. Functional relation between stimulus intensity and photically evoked cerebral responses in man. Nature (Lond). 1965; 206:720–722. [PubMed: 5832861]

Wandell, BA.; Dumoulin, SO.; Brewer, AA. Encyclopedia of Neuroscience. Elsevier; 2009. Visual Cortex in Humans; p. 251-257.

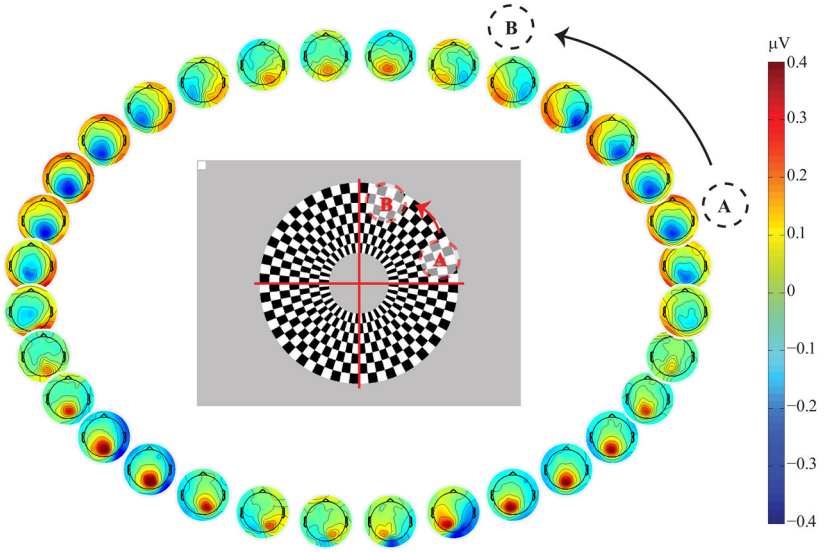

Figure 1.
topographical distributions of the earliest potential deflection “C1” (75–85 ms) in a pattern-pulse multifocal VEP derived for 32 orthogonally pulsed, radial segments of a large annular checkerboard. Example locations ‘A’ and ‘B’ of figure 2 are labeled.

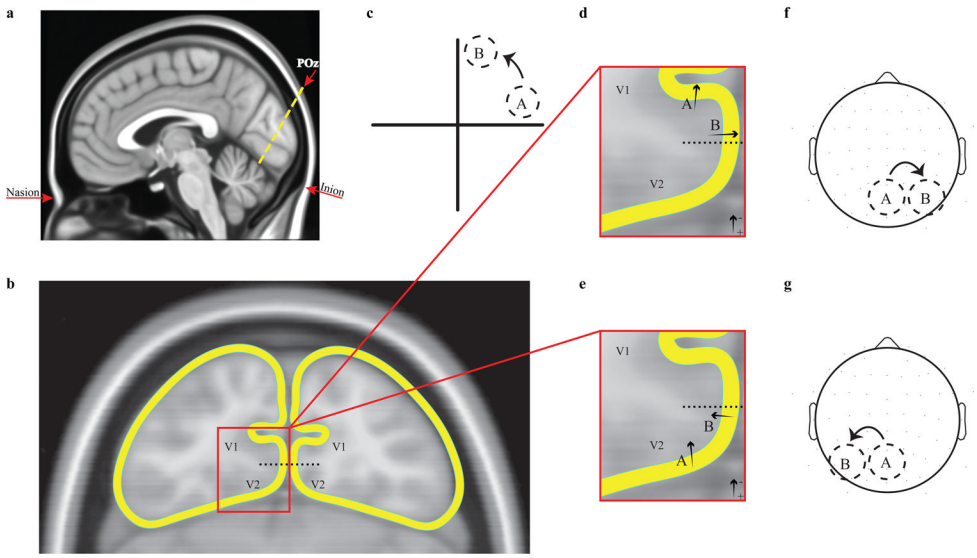

Figure 2.

a. sagittal view of the oblique coronal slice in the MNI-152 brain passing through the scalp focus of the average C1 and the average locus of functional activation for the Di Russo et al., (2002) stimulus locations. b. outline of cortical surface in this oblique coronal slice, marking the ventral V1/V2 border as mid-way down the ventral medial wall. Border location is not intended to be precise, but rather serves to illustrate orientation transitions for V1 and V2. c. example locations A and B lying close to the horizontal and vertical meridian, respectively, in the upper right field. d. A zoomed portion of the ventral left-hemisphere section of areas V1 and V2, illustrating the dipole orientation that is required to explain the scalp polarity of the C1 for location A assuming generation in **V1**, along with the rotated orientation that must follow for location B. e. The same zoomed section, illustrating the dipole orientation that is required to explain the scalp polarity of the C1 for location A assuming generation in **V2**, along with the rotated orientation that must follow for location B. In both d and e, arrows represent electrical dipoles, with the head corresponding to the negative pole. f. Topographical shift of the negative scalp focus predicted by the hypothetical V1 generators depicted in d. g. Topographical shift of the negative scalp focus predicted by the hypothetical V2 generators depicted in e. The empirically observed shifts in figure 1 match the predictions for V1 in d, f.

Table 1

salient characteristics of empirically measured C1 component topographies (Di Russo et al., 2002) listed alongside corresponding characteristics of the V1, V2 and V3 topographies simulated by Ales et al. (2013), assuming surface-negative cortical activation.

	Polarity or the scalp		**Topographic focus**	
	Upper field stimuli	**Lower field stimuli**	**Upper field stimuli**	**Lower field stimuli**
Empirical C1 (Di Russo et al 2002)	negative	positive	slightly ipsilateral	contralateral
Simulated V1	negative	positive	slightly ipsilateral	contralateral
Simulated V2	positive	negative	contralateral	slightly contralateral
Simulated V3	positive	negative	contralateral	slightly contralateral